Physical Mechanism of Laser Excited Acoustic Wave and its Application in Recognition of Incomplete-penetration Welding Defect

Yuhua Cai
School of Material Science and Engineering, Chongqing University of Technology, Chongqing 400054, People's Republic of China
Yi Luo (luoyi@cqut.edu.cn)
Chongqing University of Technology
Xinxin Wang
School of Material Science and Engineering, Chongqing University of Technology, Chongqing 400054, People's Republic of China
Shuqing Yang
School of Material Science and Engineering, Chongqing University of Technology, Chongqing 400054, People's Republic of China
Fuyuan Zhang
School of Material Science and Engineering, Chongqing University of Technology, Chongqing 400054, People's Republic of China
Fanshun Tang
School of Material Science and Engineering, Chongqing University of Technology, Chongqing 400054, People's Republic of China
Yanrui Peng
School of Material Science and Engineering, Chongqing University of Technology, Chongqing 400054, People's Republic of China

---

Research Article

Keywords: Laser pulse, Acoustic signal, Acoustic cavity, Incomplete-Penetration defect, Characteristic frequency

Posted Date: June 18th, 2021

DOI: https://doi.org/10.21203/rs.3.rs-598877/v1

Version of Record: A version of this preprint was published at The International Journal of Advanced Manufacturing Technology on April 5th, 2022. See the published version at https://doi.org/10.1007/s00170-022-09143-x.

Abstract

Incomplete penetration is a type of welding defect that severely impacts the quality of weldments. In order to identify penetration levels in pulsed laser and plasma transferred arc (laser-PTA) hybrid welding, this paper uses structure-borne acoustic sensors to detect acoustic signals. Their characteristics are then analyzed with respect to the time and frequency domains. Acoustic signals characteristic of incomplete-penetration defects were extracted using a Butterworth band-pass filter. Physical mechanisms of laser excited acoustic wave were then studied by analyzing the correlation between incomplete-penetration defects and their characteristic acoustic signals. The results showed that acoustic signals correlating to incomplete-penetration defects have characteristic frequencies ranging from 0 to 10 kHz, which are generated by interaction between the pulsed laser beam and molten pool. An incomplete-penetration defect constitutes an acoustic cavity, which is an acoustic transmission structure. The structure of phonation sources and the acoustic cavity are affected by levels of penetration, giving rise to acoustic signals with different characteristics. In general, the study of physical mechanisms of laser excited acoustic wave lays a foundation for on-line identification of incomplete-penetration defects in laser-PTA hybrid welding.

Introduction

Hybrid laser-arc welding was first proposed by Steen in the late 1970s [1]. Hybrid laser-arc welding combines a laser beam with high energy density and an electric arc with large heat input. Their high efficiency, high stability and low distortion make them far superior to pure laser welding and pure arc welding [2–4]. Hybrid laser-arc welding has been widely applied in machinery manufacturing, aerospace, rail transit and many other fields [5]. The full penetration of the weld during the welding process is fundamental to ensuring the quality of the joint. Accordingly, penetration level is critical to the quality of the weld [6]. Non-destructive testing and destructive testing are the most commonly used methods for inspecting weld quality. Generally, post-welding non-destructive testing is used to check for weld penetration defects. As modern industry strives towards more efficient forms of production, on-line identification of weld penetration in hybrid laser-arc welding has become a key technology and major research direction in welding automation. As such, this field has drawn the attention of many scholars.

Previous studies have proposed some on-line methods for measuring penetration levels. Acoustic wave signals and visual images are the most common means of weld quality assessment. Lü et al. [7] built a linear model that relates arc acoustic signal to arc length with respect to pulsed Gas Tungsten Arc Welding (GTAW), allowing precise prediction of the arc length to more accurately measure penetration levels and weld quality. Wang et al. [8] collected acoustic wave signals during plasma arc welding using a condenser microphone. Their experimental results showed that changes of the signal power spectrum can adequately reflect weld penetration levels. Liu et al. [9] proposed the use of trained neural networks to process information on the properties of arc acoustic signals during the welding process. This technique can efficiently achieve penetration recognition. Wu et al. [10] introduced signal acquisition methods that are based on visual and acoustic sensors. Their hybrid processing method successfully identified penetration levels during the plasma arc welding process. Liang et al. [11] used 3D vision sensors to collect images of the surfaces of weld pools in GTAW welding and proposed a support vector regression model to overcome the shortcomings of traditional neural networks, which require large amounts of training data. This allowed their method to more effectively measure weld penetration levels. Song et al. [12] analyzed acoustic signal characteristics in non-keyhole, keyhole and cutting modes during plasma arc welding and built a system for measuring penetration levels to an accuracy of 93.23%. Lü et al. [13] trained a typical back propagation artificial neural network prediction model based on the characteristics of acoustic signals generated during pulsed GTAW welding. This method was able to predict penetration levels to an accuracy of 80–90%. Wu et al. [14] used images of the back keyhole of the workpiece to build an Adaptive Network Fuzzy Inference System for monitoring weld penetration during plasma arc welding. These methods have been successful in identifying penetration levels.

A literature review shows that many studies have used airborne acoustic signals to measure penetration levels. However, airborne sensors for acoustic signals are relatively inefficient. The noise signal in the environment has a strong interference on the penetration acoustic signal. Structure-borne sensors are able to obtain more information from acoustic signals [15]. The structure-borne acoustic sensing method can greatly improve the anti-interference ability to environmental noise and the detection ability to useful acoustic signal. It can meet the conditions for large-scale use in the welding industry because of the advantages of low cost, high efficiency and strong versatility. In order to obtain detailed information on penetration levels during pulsed laser and plasma transferred arc (laser-PTA) hybrid welding, the present paper used structure-borne acoustic sensors to measure weld penetration. We examine how laser-PTA hybrid welding arising from incomplete penetration can be identified through an analysis of characteristic acoustic signals, thereby promoting the development of systems for measuring penetration levels.

Experiment Details

A laser-PTA hybrid welding system was used in the experiment, as illustrated in Fig. 1a. The welding heat source is composed of a continuous plasma arc and a pulsed Nd:YAG laser beam that act in tandem on the molten weld pool. A plasma plume is generated during the interactions between the laser beam, plasma arc and molten weld pool. A system for monitoring acoustic signals in real time was used during the laser-arc hybrid welding experiment. Figure 1b shows the schematic of this laser-PTA hybrid welding experiment. The experiment used structure-borne sensors to reduce the attenuation of acoustic energy during the transmission process and prevent interference from environmental noise. In order to reduce reflection and attenuation of structure-borne acoustic signal at the interface, a vacuum silicone grease couplant was applied evenly on the contact surface between the sensor and the workpiece. A structure-borne acoustic sensor was installed on the workpiece surface more than 50 mm away from the molten weld pool to ensure the sensing signal strength and avoid the damage caused by spatter. The propagation velocity of sound wave in solid steel is up to 3000m/s-6000m/s. The signal delay caused by the distance between the sensor installation position and the molten pool is only a few microseconds. Therefore, regardless of the attenuation and the time delay of the acoustic emission signal in stainless steel. It is considered that the relative position change of the sensor and the molten pool does not affect the characteristics of the detected acoustic signal.

The sensors used in experiment are structure-borne, there is little attenuation of acoustic energy transmitted through solids. Due to the high propagation speed of structure-borne acoustic wave in solid, the position change caused by laser heat source movement will not bring unacceptable time delay of acoustic signals. Therefore, the sensors are not affected by changes in installation position. During the experiments, all data on laser-induced acoustic excitations were extracted and analyzed. Acoustic signals collected during the welding process are amplified by the preamplifier, filtered by the signal processor, and sent to the computer through the data acquisition unit (ART PCI-8757) for further processing and analysis. Sampling rates in the experiments were set to 150 kHz based on the Nyquist criterion (Zhao et al. 2020). LabVIEW, a sampling and analysis software developed by National Instruments, is used to acquire data and further analyze the acoustic signals. Table 1 shows the welding parameters used in the experiments, which used 304 stainless steel plates with a thickness of 2 mm, 3 mm, and 6 mm respectively. During the welding process, the fixture is used to keep the assembly gap of the workpiece at 0.3mm, so that the research conditions are consistent with the assembly accuracy of the production conditions. Gaseous argon was used as both the plasma gas and the shielding gas. The same peak laser power levels and other pulse parameters are used in each experiment. Penetration levels were measured based on changes in welding speed and arc current. In particular, arc current was lowered for 6 mm plates as it was necessary to achieve incomplete penetration. However, arc current applied to 3-mm workpieces were increased to 80 A to ensure their complete penetration under the experimental conditions.

Table 1
Welding parameters used in experiment.

No.	Workpiece thickness *d* / mm	Welding speed *v* / mm·s⁻¹	Laser pulse frequency *f* / Hz	Arc current *I*/A	Laser pulse power P_m / kW	Laser pulse duration T_w / ms
1	2	4	100	40	3	2
2	2	5	100	40	3	2
3	2	7	100	40	3	2
4	6	4	100	60	3	2
5	6	5	100	60	3	2
6	6	7	100	60	3	2
7	3	3	100	80	3	2
8	3	5	100	80	3	2
9	3	7	100	80	3	2
10	3	9	100	80	3	2

Results And Discussion

3.1 Acoustic signal characteristics

In order to obtain different weld penetrations, the welding currents for 2-mm plates and 6-mm plates were respectively 40 A and 60 A, while other parameters were maintained at a constant level (welding speed 4 mm/s, laser frequency 100 Hz, peak power 3 kW, pulse duration 2 ms). Figure 2 shows the weld cross-section morphology and the acoustic signals detected during the welding process. It can be observed that the 2-mm plate was fully penetrated while the 6-mm plate was only partially penetrated. In other words, there is no penetration defect in the 2-mm plate while there are significant incomplete-penetration defects in the 6-mm plate. However, an ocular observation of the time-domain characteristics of the acoustic signals in Fig. 2 yields no significant features that indicate the presence of defects. Therefore, it is not enough to merely analyze acoustic signals in the time domain.

In order to study the differences in acoustic signals for different penetration levels, we welded 2-mm-thick and 6-mm-thick plates at speeds of 4 mm/s, 5 mm/s, and 7 mm/s, respectively. Acoustic signals were collected in real time during the welding process. Weld cross-section morphologies and signals in the time domain are shown in Fig. 3. In addition, the components of these acoustic signals are displayed in the frequency domain (0–60 kHz) through an analysis of the self-power spectrum. The results for 2-mm-thick plates show that welds are fully penetrated when welding speed is 4 mm/s or 5mm/s. The weld reaches a critical penetration state when the welding speed is 7 mm/s. For 6-mm-thick plates, results show that all welds are in a state of incomplete-penetration. By observing the characteristic spectral lines in the frequency domain, we can see that there are four frequency components that should be noted. These spectral lines occur near frequencies of 57 kHz, 37 kHz, 20 kHz, as well as at frequencies below 10kHz, as shown in Fig. 3. The characteristic spectral lines near frequencies of 57 kHz and 37 kHz are not closely related to incomplete-penetration defects. In contrast, the spectral lines near frequencies of 20 kHz and below 10 kHz are suspected to be related to incomplete-penetration defects. This is especially the case for signal compositions with frequencies below 10 kHz. In the case of full-penetration welds, such as in the 2-mm plates, there are almost no signal components with frequencies below 10 kHz. For incomplete-penetration welds, such as in the 6-mm plates, we observe many signal components and a strong signal intensity at frequencies below 10 kHz. Figure 4 shows a clearer analysis of the results with respect to the frequency domain. This indicates the need for special analysis of acoustic signals in these two frequency bands.

Characteristic frequency domains of these two frequency bands are subdivided as shown in Fig. 4. According to the distribution of acoustic signals in the frequency domain below 10 kHz, the lower cut-off point is set at 3 kHz and the higher cut-off point is set at 7 kHz. For signals near the characteristic spectral line at 20 kHz, a narrower characteristic frequency band is set so that signal characteristics for different welding speeds can be analyzed more accurately.

Next, a Butterworth band-pass filter was used to extract these characteristic signals. For the full-penetration welds in 2-mm plates, very little information on their features could be extracted from the acoustic signals. It can be seen from Fig. 5a that, when the welding speed is 4mm/s, almost no characteristic signal information of value can be extracted. This holds true for frequency bands from 3 kHz to 7 kHz and around 20 kHz. An analysis of self-power spectrums, illustrated in Fig. 3a, shows no distribution of signal components in these two frequency bands. At welding speeds of 5 mm/s or 7 mm/s, increases in welding speed affect weld penetration levels, but the welds remain at full or critical penetration. Although some acoustic signal components were extracted, these extracted signals have fewer event characteristics.

Characteristic signals extracted from welds in 6-mm plates are also different from those from 2-mm plates due to significant differences in their penetration levels. Figure 5 shows the acoustic signals extracted in characteristic frequency domains. The acoustic signals extracted by filtering in the frequency band near 20 kHz also have fewer event characteristics. However, acoustic signals extracted in the 3 kHz to 7 kHz frequency band have characteristics that are different from each of the extracted signals mentioned above, the difference being that these extracted acoustic signals have obvious event characteristics: signal pulses appear in clusters to form an “acoustic event”. Figure 6 highlights the features of these acoustic events in the time domain. It is clear that the frequencies of these acoustic events are analogous to those of laser pulses, indicating that these extracted acoustic events were generated by pulse laser excitation. This phenomenon is present only in acoustic signals from incomplete-penetration welds.

From the above analysis, it can be determined that signal frequencies lower than 10 kHz constitute a signal frequency band characteristic of incomplete-penetration defects. The following section will analyze the mechanisms underlying the generation of these characteristic signals.

3.2 Physical mechanism of laser excited acoustic wave

Figure 7 shows a schematic of phonation sources in a molten pool. Sources of phonation are constituted by certain physical processes during the course of welding, such as the electromagnetic effects of the plasma arc, energy coupling between the laser beam and the plasma arc, liquid-phase convection in the molten pool, plasma gas flow or recoil force in the keyhole, and so on. These physical phonation sources produce acoustic signals with different frequency characteristics, as well as different characteristic spectral lines in the self-power spectrum (as shown in Fig. 3). An intense plasma eruption effect is generated in the keyhole when a laser beam with a high energy density acts on the molten pool. The plasma then generates a downward recoil force on the bottom of the molten pool, causing it to vibrate at a unique frequency. Weld penetration level can be determined by this unique vibration frequency, which is closely related to the action process of the laser beam. Therefore, sources of phonation for incomplete-penetration defects are caused by interaction between laser energy and the molten pool. Accordingly, the frequency of acoustic events extracted in the frequency band below 10 kHz (characteristic frequency band of incomplete-penetration defect) will be the same as that of laser pulses as shown in Fig. 6.

The incomplete-penetration defect is at the bottom of the molten pool. The propagation of acoustic signals from incomplete-penetration defects is closely related to the acoustic transmission structure of defective welds. An incomplete-penetration defect is an acoustic transmission structure – an acoustic cavity. Figure 8 shows the physical structure and acoustic transmission characteristics of an acoustic cavity.

A low penetration depth implies that the molten pool has a lower volume while the weld structure has a larger incomplete-penetration defect, which creates a large acoustic cavity, as shown in Fig. 8a. In this structure, the acoustic cavity acts like a loudspeaker, amplifying the acoustic signals from various phonation sources in the molten pool. At the same time, the acoustic wave resonates at a relatively low frequency in the large acoustic cavity. This creates acoustic signals characteristic of incomplete-penetration defects. Because of the small volume of the molten pool, the recoil force generated by laser pulse energy in the molten pool can almost directly impact its bottom, and generate a significant vibration effect. On this condition, the frequencies of these acoustic vibration events are analogous to those of laser pulses as shown in Fig. 6. The acoustic cavity of an incomplete-penetration defect is obviously more conducive to the amplification of these types of oscillating wave. In Fig. 8a, this characteristic oscillation wave is denoted “AW”, while acoustic waves from other phonation sources are denoted “AW’”. In other words, when an incomplete-penetration defect is present, acoustic waves characteristic of defects are more readily amplified by the acoustic cavity, thus displaying a relatively low signal frequency.

A deeper penetration level means that the molten pool has a larger volume while the incomplete-penetration defect in the weld structure is smaller, which creates a relatively small acoustic cavity, as shown in Fig. 8b. Accordingly, the acoustic cavity will have a weaker resonance effect and a weaker amplification effect on acoustic waves from various phonation sources. At the same time, the larger molten pool will have a buffering effect on acoustic oscillation generated by interaction between laser energy and the molten pool. These factors weaken the acoustic wave AW correlating to incomplete-penetration defects.

For full-penetration welds, the molten pool has the largest volume. Obviously, because the "size" of an incomplete-penetration weld defect is zero, the acoustic cavity does not exist, as shown in Fig. 8c. Because of the large volume of the molten pool, recoil force generated by laser pulse energy in the keyhole can barely directly impact the bottom of molten pool. The laser energy generates an oscillation in the molten pool. At the same time, the large volume of the molten pool has a significant buffering effect on acoustic oscillation generated by interaction between the laser energy and molten pool, which greatly compresses the volume of the acoustic cavity. Thus, acoustic waves are not amplified by the acoustic cavity. Thus, there is barely any sign of the acoustic wave AW correlating to incomplete-penetration defects. The small assembly clearance remaining at the bottom of the weld is similar to a small acoustic cavity, which tends to produce high frequency acoustic waves. Therefore, there is no sign of low frequency components below 10 kHz in the acoustic signal self-power spectrum that correspond to full-penetration welds (as shown in Fig. 3a).

The above analysis of the physical mechanisms of laser excited acoustic wave has been experimentally verified through welding experiments on 2-mm and 6-mm plates (as shown in Figs. 3 to 5). Further welding experiment results for 3-mm plates are shown in Figs. 9 and 10.

As shown in Fig. 9, welds attain full penetration when welding speed is 3 mm/s. There are almost no signal components with frequencies below 10 kHz in the corresponding self-power spectrum. Depth of weld penetration gradually decreases as welding speed increases from 3 mm/s to 9 mm/s. As penetration depth decreases, the depth of an incomplete-penetration defect (h') increases from 0 to 2.20 mm, as shown in Fig. 10. Increases in incomplete-penetration depth indicate larger acoustic cavities in the weld structure. Accordingly, as per our previous analysis, there will be more significant acoustic signal components with frequencies below 10kHz (as shown in Fig. 9), which are then extracted as shown in Fig. 10. It can be seen that the frequencies of acoustic events in the extracted signal are entirely consistent with the frequencies of laser pulses. At the same time, the amplitude intensity of acoustic events increases gradually with increases in the depth of incomplete penetration. The experimental results in Fig. 9 and Fig. 10 support our hypothesis of the physical mechanisms of vocalization during the occurrence of incomplete-penetration defects. In general, the physical mechanisms of vocalization lay a foundation for on-line identification of incomplete-penetration defects in laser-PTA hybrid welding.

Conclusion

(1) Acoustic signals correlating to incomplete-penetration defects have a characteristic frequency domain of 0 to 10 kHz. Acoustic signal components appearing in the characteristic frequency domain indicate the occurrence of incomplete-penetration defects in laser-PTA hybrid welding. When an incomplete-penetration defect occurs during the welding process, characteristic acoustic signals are generated interaction between the pulsed laser beam and molten pool, which are composed of acoustic events with the exact same frequencies as those of the laser pulse.

(2) The interaction between the laser beam and molten pool produces a downward recoil force at the bottom of the molten pool, which causes it to vibrate at a unique frequency. This vibration effect produces a phonation source associated with incomplete-penetration defects, which are acoustic transmission structures that this paper describes as acoustic cavities. An acoustic cavity is similar to a loudspeaker, with an acoustic transmission function of amplifying acoustic waves and causing them to generate a resonance effect.

(3) The structure of phonation sources and acoustic cavities are affected by different states of penetration. Large incomplete-penetration defects are correlated with large acoustic cavities, which create a more significant amplification effect on acoustic signals correlating to such defects. In relatively small molten pools, it is easier for laser pulse energy to generate vibrations that in turn produce acoustic signals correlating to defects. When incomplete-penetration defects are relatively small, acoustic cavities have a weaker amplification effect on acoustic signals correlating to defects. In the case of full penetration, there is no acoustic cavity, while the large molten pool has a significant buffering effect on laser-generated acoustic oscillations. Accordingly, acoustic signals correlating to defects are generally non-existent. On-line identification of incomplete-penetration defects in laser-PTA hybrid welding is made possible by these acoustic transmission characteristics.

Declarations

Acknowledgements

This work was supported by Basic Science and Frontier Technology Research Project of Chongqing Science and Technology Commission of China (Grant No.cstc2017jcyjBX0065) and Science and Technology Research Program of Chongqing Education Commission of China (Grant No. KJZD-M202001102).

Conflicts of interest

We declare that we have no financial and personal relationships with other people or organizations that can inappropriately influence our work, there is no professional or other personal interest of any nature or kind in any product, service and/or company that could be construed as influencing the position presented in, or the review of, the manuscript entitled “Physical mechanism of laser induced acoustic wave and its application in recognition of incomplete-penetration welding defect”.

Availability of data and material

Not applicable

Code availability

Not applicable

Ethics approval

Not applicable

Consent to participate

Written informed consent for participation was obtained from all participants.

Consent for publication

Written informed consent for publication was obtained from all participants.

Authors' contributions

Yuhua Cai performed the data analyses and wrote the manuscript;

Yi Luo contributed to the conception of the study;

Xinxin Wang contributed significantly to analysis and manuscript preparation;

Shuqing Yang performed the experiment;

Fuyuan Zhang helped perform the analysis with constructive discussions;

Fanshun Tang performed the experiment;

Yanrui Peng helped perform the analysis with constructive discussions.

References

[1] Steen W. Arc augmented laser processing of materials. Journal of applied physics, 1980, 51(11): 5636–5641.

[2] Hu B, den Ouden G. Synergetic effects of hybrid laser/arc welding. Sci Technol Weld Join, 2013, 10(4): 427-431.

[3] Xiao R, Wu S. Research progress in laser arc hybrid welding. China Laser, 2008, 35(11): 1680-1685.

[4] Bappa A. Hybrid laser arc welding: State-of-art review. Optics & Laser Technology, 2018, 99: 60-71.

[5] Morten K, Farhang F, Ewa K, Sigurd V. Application of Hybrid Laser arc Welding for the Joining of Large Offshore Steel Foundations. Physics Procedia, 2017, 89: 197-204.

[6] Allen C, Verhaeghe G, Hilton P, Heason C, Prangnell P. Laser and hybrid laser-MIG welding of 6.35 and 12.7mm thick aluminium aerospace alloy. Materials Science Forum, 2006, 519-521: 1139-1144.

[7] Lu N, Zhong J, Chen H, Lin T, Chen S. Real-time control of welding penetration during robotic GTAW dynamical process by audio sensing of arc length. The International Journal of Advanced Manufacturing Technology, 2014, 74: 235-249.

[8] Wang Y, Zhao P. Noncontact acoustic analysis monitoring of plasma arc welding. International Journal of Pressure Vessels and Piping, 2001, 78: 43-47.

[9] Liu L, Lan H, Zheng H. Feature evaluation and selection of penetration arc sound signal based on neural network. Transactions of the China Welding Institution, 2010, 31(3): 25-28.

[10] Wu D, Huang Y, Chen H, He Y, Chen S. VPPAW penetration monitoring based on fusion of visual and acoustic signals using t-SNE and DBN model. Materials & Design, 2017, 123: 1-14.

[11] Liang R, Yu R, Luo Y, Zhang Y. Machine learning of weld joint penetration from weld pool surface using support vector regression. Journal of Manufacturing Processes, 2019, 41: 23-28.

[12] Song S, Chen H, Lin T, Wu D, Chen S. Penetration state recognition based on the double-sound-sources characteristic of VPPAW and hidden Markov Model. Journal of Materials Processing Technology, 2016, 234: 33-44.

[13] Lv N, Xu Y, Li S, Yu X, Chen S. Automated control of welding penetration based on audio sensing technology. Journal of Materials Processing Technology, 2017, 250: 81-98.

[14] Wu D, Chen H, Huang Y, He Y, Hu M, Chen S. Monitoring of weld joint penetration during variable polarity plasma arc welding based on the keyhole characteristics and PSO-ANFIS. Journal of Materials Processing Technology, 2017, 239: 113-124.

[15] Luo Y, Zhu L, Han JT, Xie XJ, Wan R, Zhu Y. Study on the acoustic emission effect of plasma plume in pulsed laser welding. Mechanical Systems and Signal Processing, 2019, 124: 715-723.

Figures

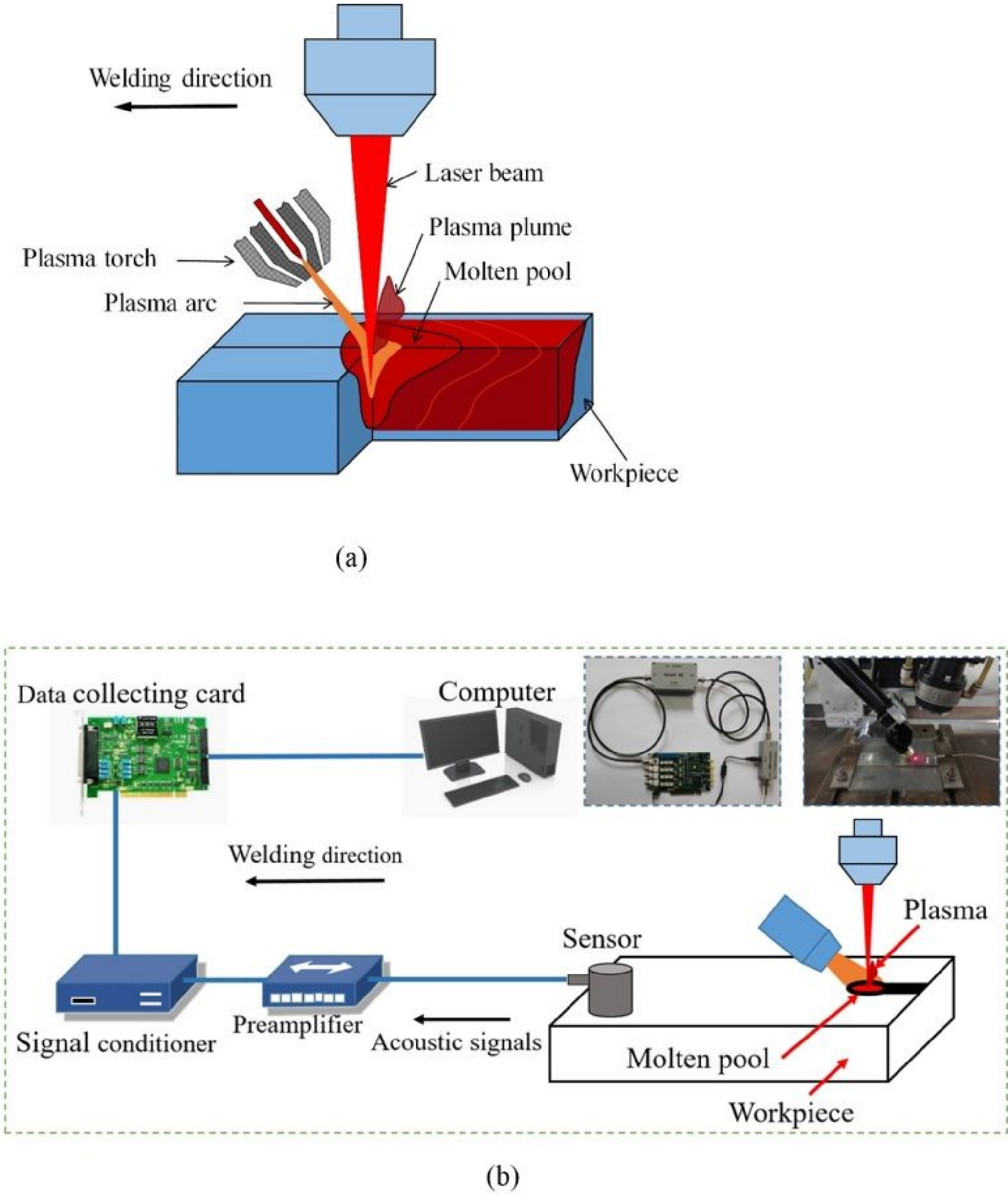

Figure 1

Schematic of (a) welding process and (b) acoustic signal monitoring system in laser-arc hybrid welding.

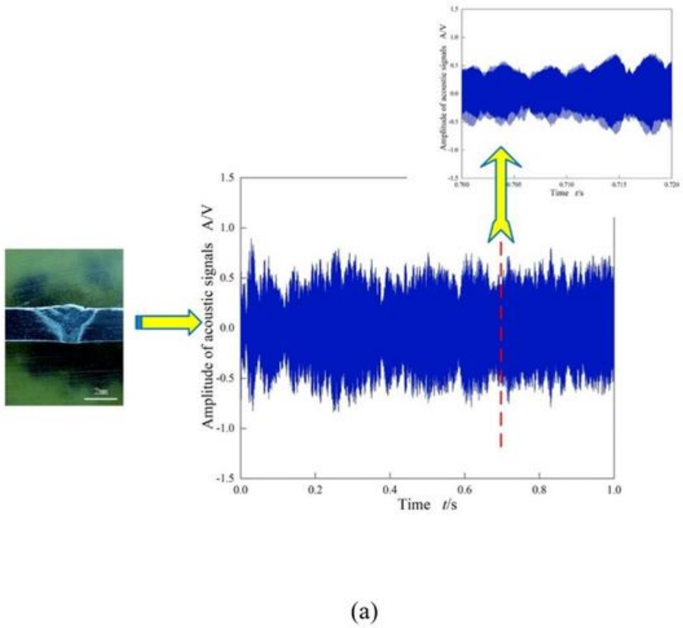

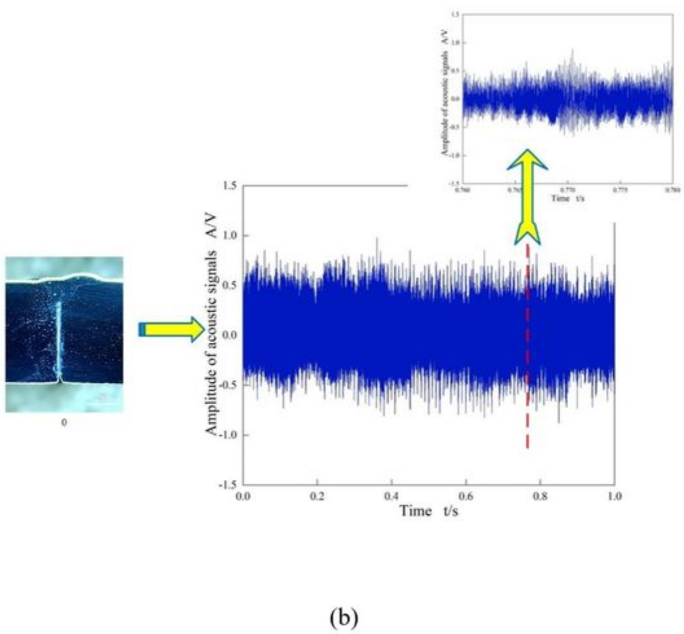

Figure 2

Weld cross-section morphology and acoustic signals of (a) 2mm and (b) 6mm thickness plate.

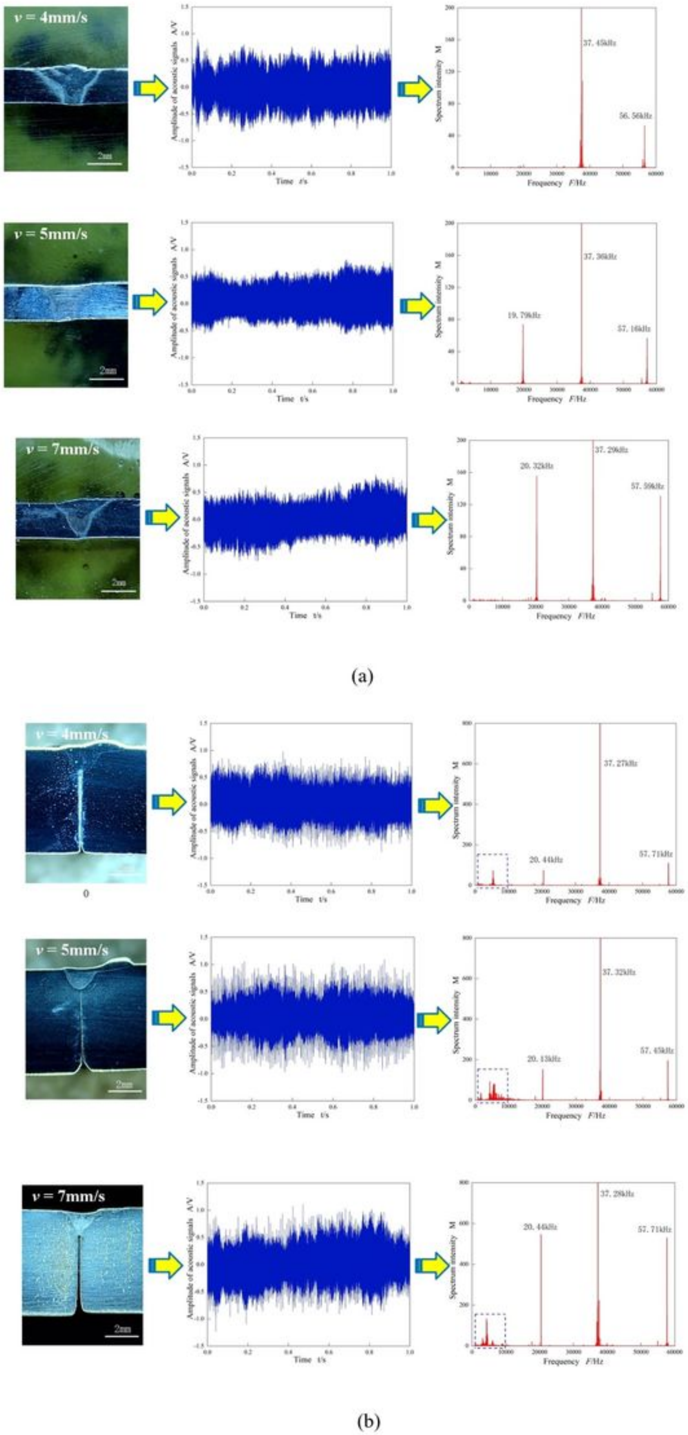

Figure 3

Characteristics of acoustic signals detected under different welding speeds for (a) 2mm thickness plate and (b) 6mm thickness plate.

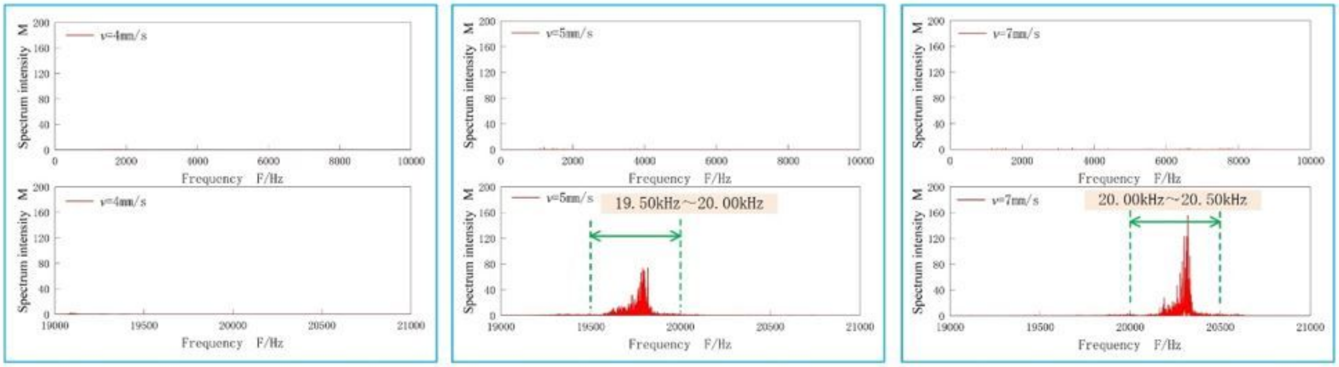

(a)

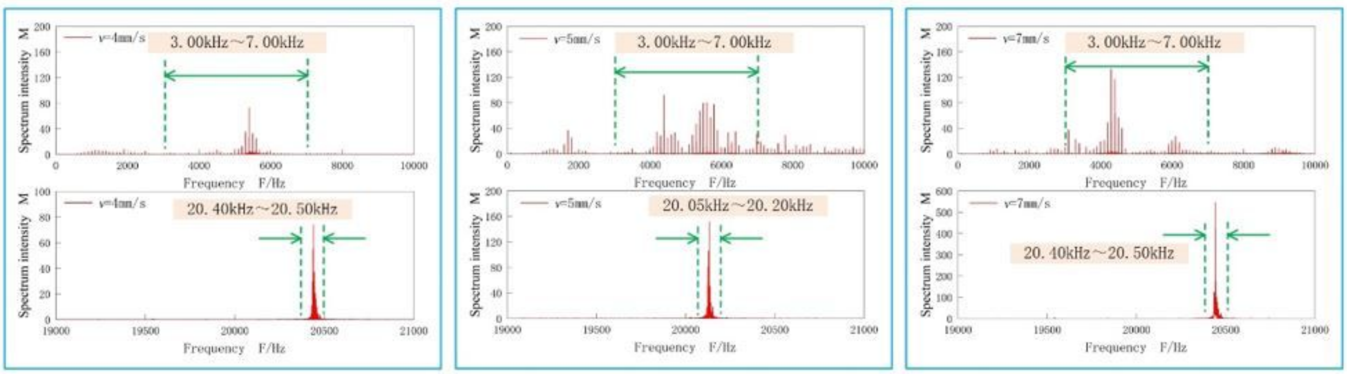

(b)

Figure 4

Characteristic frequency domain of acoustic signals detected under different welding speeds for (a) 2mm thickness plate and (b) 6mm thickness plate.

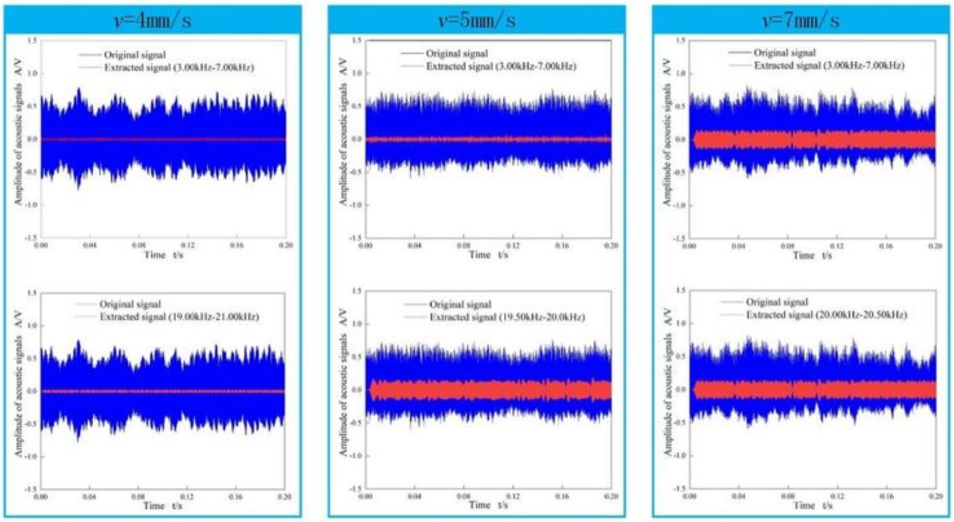

(a)

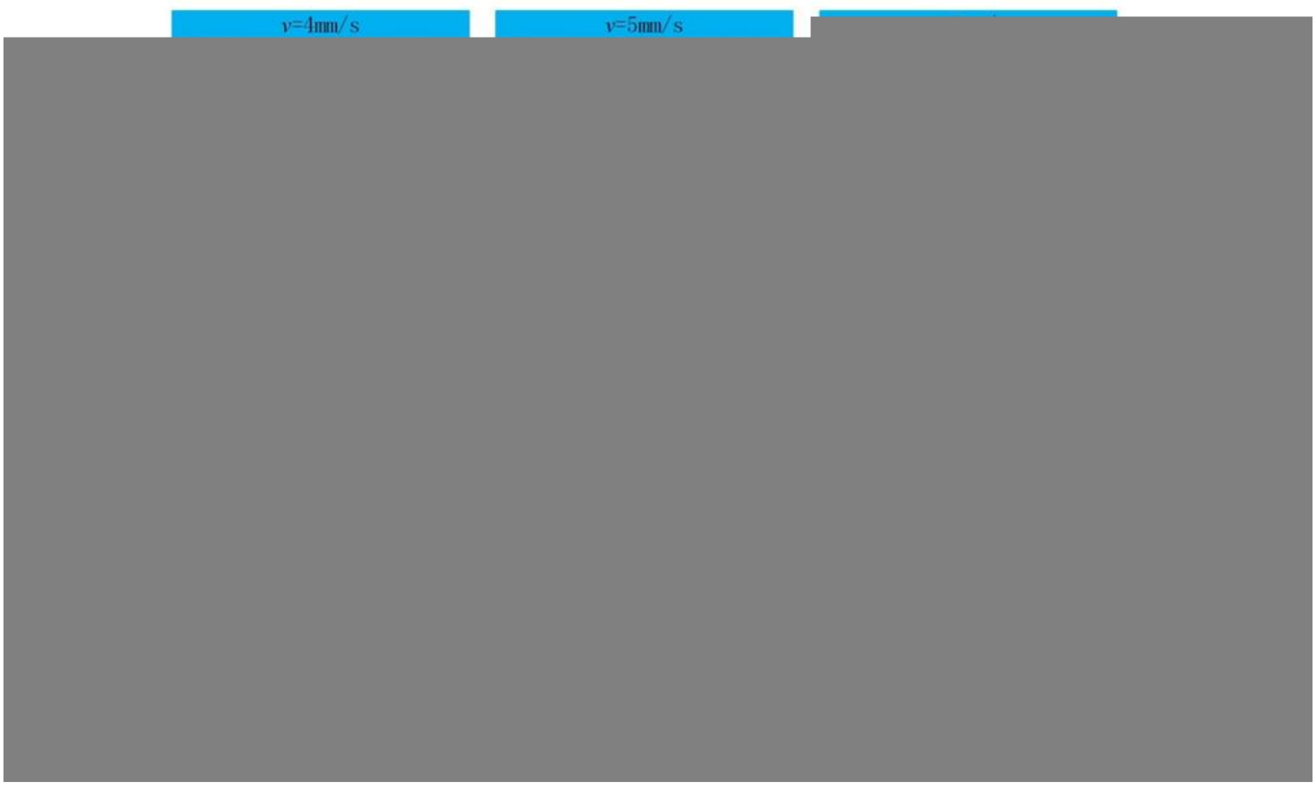

Figure 5

Extraction of acoustic signals in characteristic frequency domain for (a) 2mm thickness plate and (b) 6mm thickness plate.

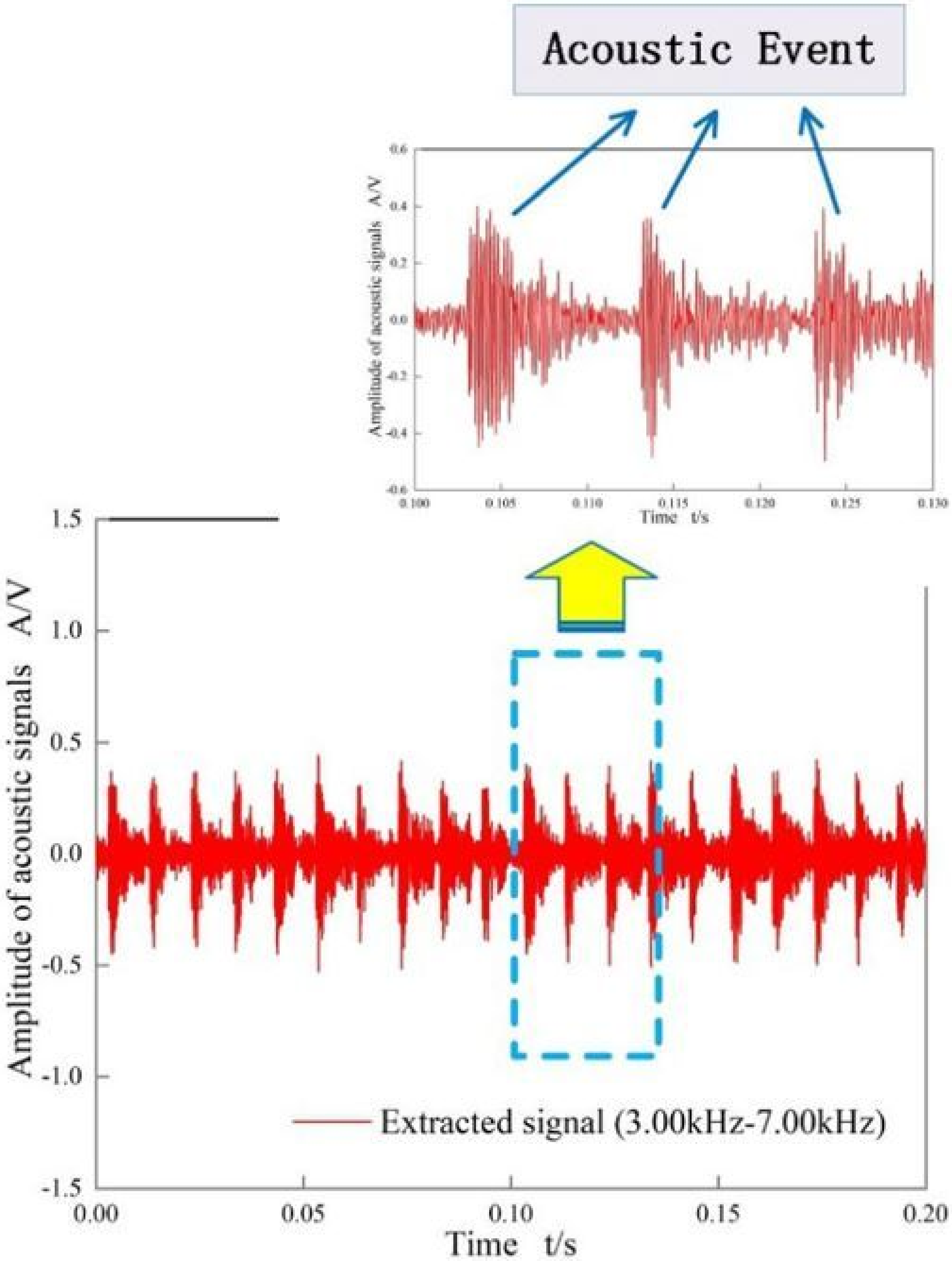

Figure 6

Acoustic events in acoustic signals.

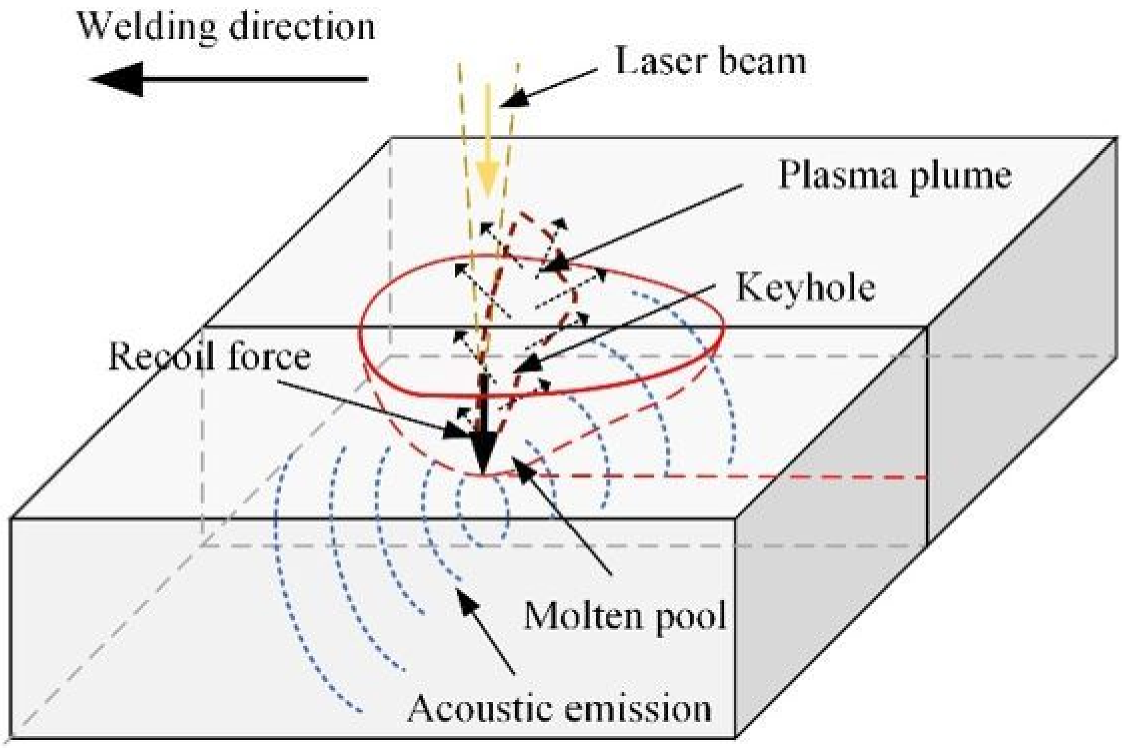

Figure 7

Schematic of phonation source in molten pool.

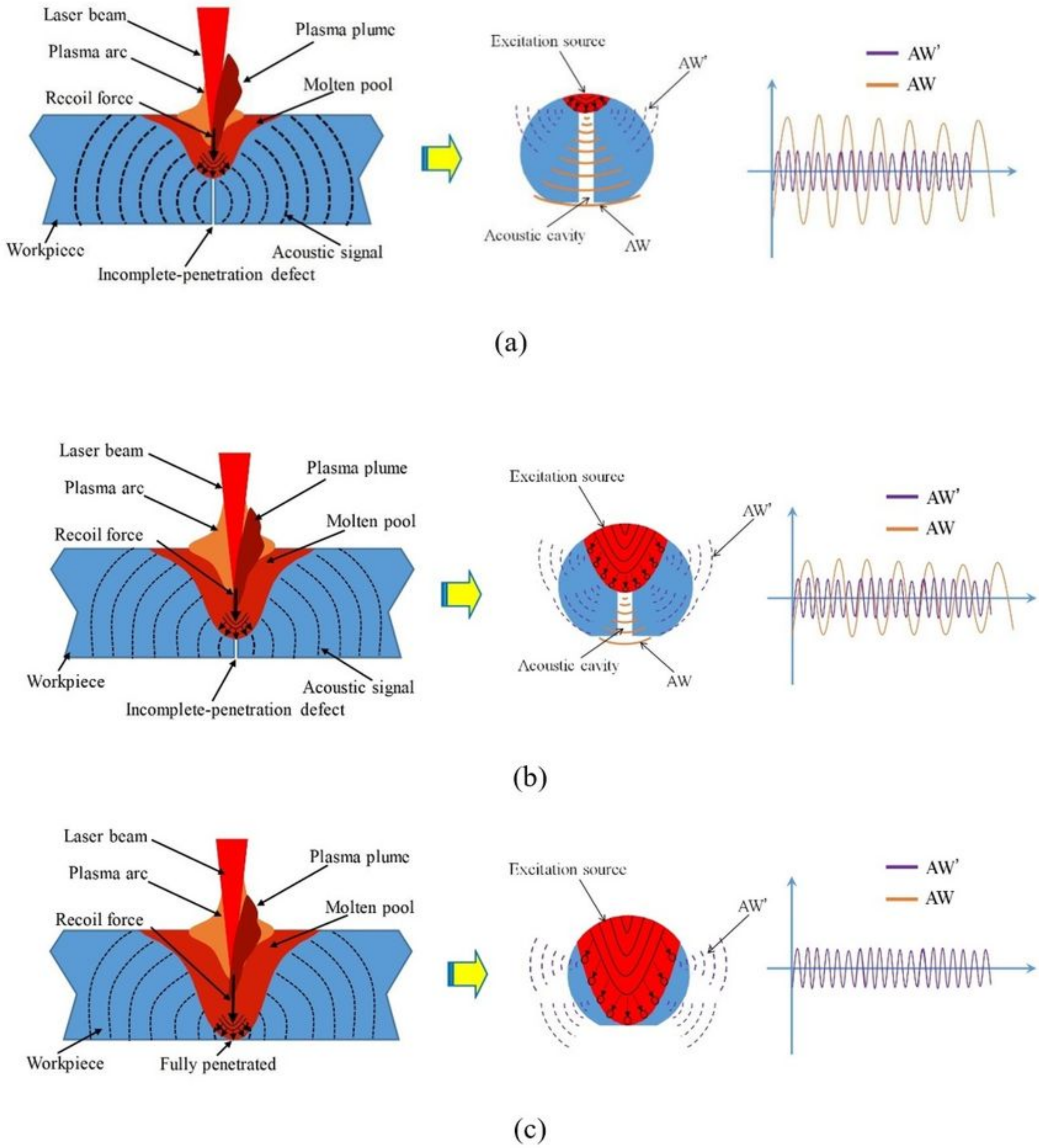

Figure 8

Physical structure and acoustic transmission characteristics of acoustic cavity under (a) low penetration, (b) deep penetration and (c) fully penetration status.

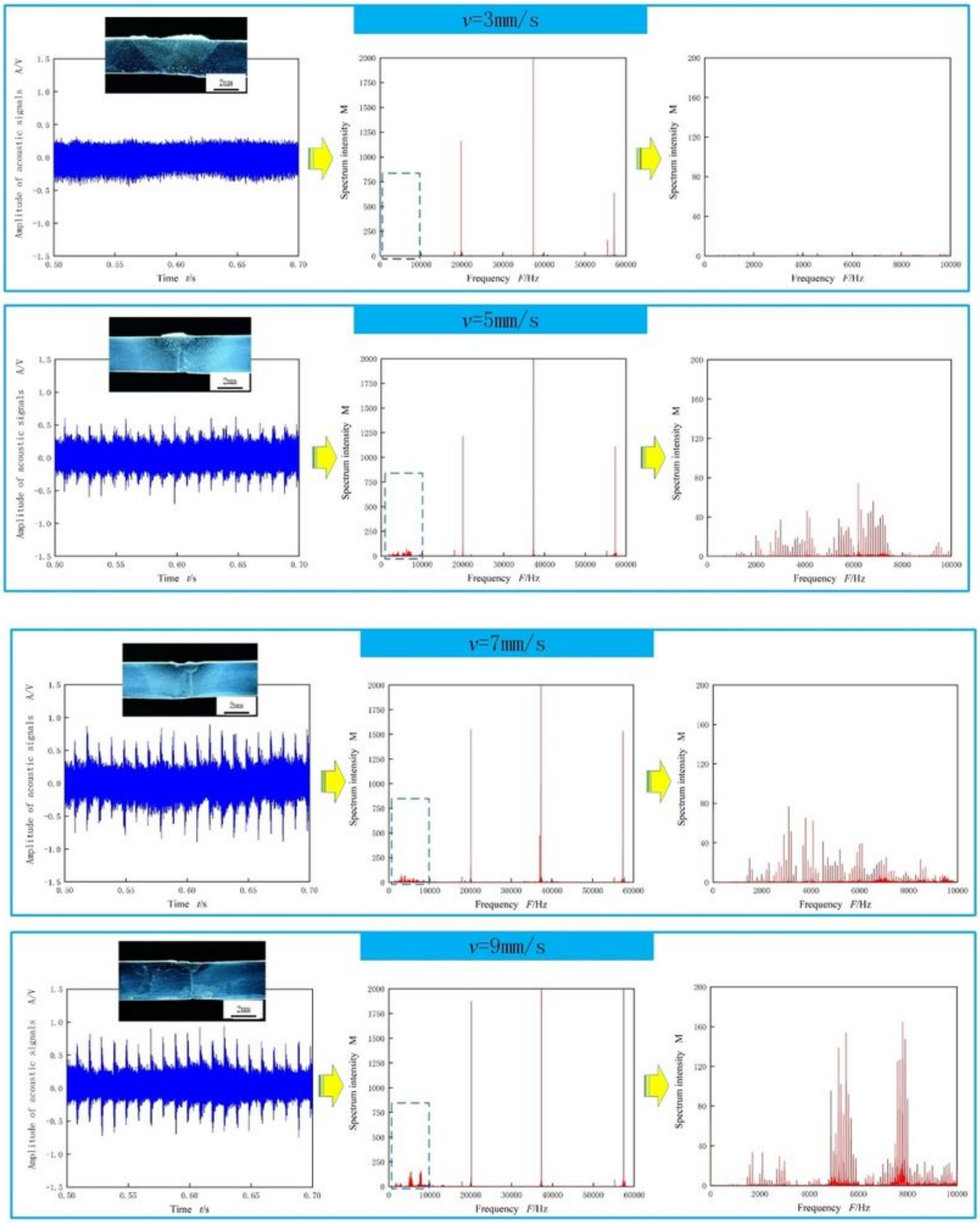

Figure 9

Penetration state, original acoustic signal and its characteristic frequency domain for 3mm thickness plate under different welding speed.

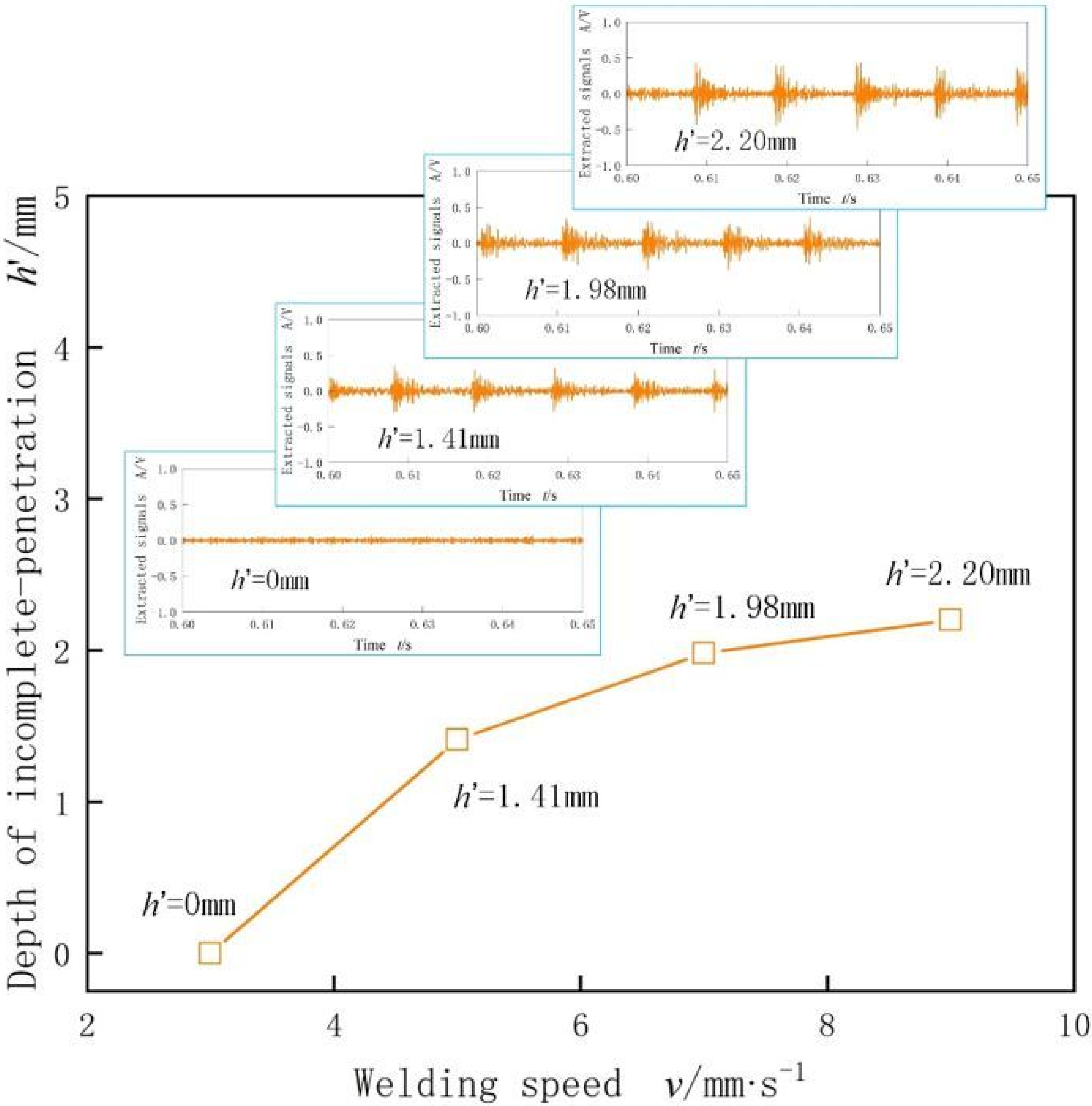

Figure 10

Relationship of incomplete-penetration depth and characteristic acoustic signal intensity.